Article

Fibril-Forming Organelles in Mesangial Cells in Renal Biopsies from Patients with Light-Chain-Associated Amyloidosis

Guillermo A. Herrera [1,]*, Jiamin Teng [1], Chun Zeng [1], Luis Del Pozo-Yauner [1], Bing Liu [1] and Elba A. Turbat-Herrera [2]

[1] Frederick P. Whiddon College of Medicine, University of South Alabama, 2451 University Hospital Dr., Mobile, AL 36617, USA; jteng@health.southalabama.edu (J.T.); czeng@health.southalabama.edu (C.Z.); ldelpozoyauner@health.southalabama.edu (L.D.P.-Y.); bingliu@health.southalabama.edu (B.L.)

[2] Mitchell Cancer Center, University of South Alabama, 1660 SpringHill Ave, Mobile, AL 36604, USA; etherrera@health.southalabama.edu

* Correspondence: gherrera@health.southalabama.edu; Tel.: +1-251-471-7719; Fax: +1-251-471-7715

Abstract: The process of light-chain-associated amyloid (AL-Am) fibril formation in unique organelles (fibril-forming organelles) with lysosomal features has been documented in vitro in renal mesangial cells incubated with amyloidogenic light chains using electron microscopy and lysosomal gradient centrifugation to visualize intricate interactions between monoclonal light chains and endosomes/lysosomes. It is important to determine whether this process also occurs in vivo in the human renal mesangium. The present study analyzes 13 renal biopsies from patients with renal AL-amyloidosis and utilizes ultrastructural labeling techniques to define the nature and function of these organelles. Organelles were labeled for lysosomal-associated membrane protein (LAMP) and CD-68 (a macrophage marker). Furthermore, lambda was also localized inside these structures in transformed mesangial cells with a macrophage phenotype. These 11 cases from renal biopsies with a diagnosis of AL-amyloidosis (5 kappa and 8 lambda light-chain-associated) were examined ultrastructurally. All of the cases exhibited numerous fibrils forming organelles in approximately 40–50% of the remaining mesangial cells. All of the cases revealed mesangial cells engaged in active amyloidogenesis. Fibril-forming organelles are organelles with morphological/immunohistochemical and biochemical characteristics of lysosomes but with a unique, peculiar morphology. Five cases of other glomerular disorders used as controls were also carefully scrutinized for fibril-forming organelles and failed to show any. In the AL-amyloid renal cases, there was an intricate interaction between the fibril-forming organelles and lambda-/kappa-containing amyloid fibrils, supporting the notion that the monoclonal light chains participated in their formation.

Keywords: AL-amyloidosis; mesangial cells (MCs); monotypical light chains; fibril-forming organelles; kidney; mesangium

1. Introduction

Amyloidogenesis is a complex, multi-step process that has been elucidated with details in experimental models [1–4]. The information obtained needs to be translated to human material. There are more than 46 precursor proteins associated with amyloidosis [5]. The most common form of amyloidosis in the Western world is light-chain-associated amyloidosis (AL-amyloidosis).

While the mechanism of amyloid formation may differ somewhat from organ to organ depending on the cell types involved and the amyloid type, it is likely that a common denominator exists. Amyloid formation in the renal mesangium has been carefully delineated [1,2,6], and the translation of this information into renal biopsies is important to test whether the same mechanisms are involved.

In 1975, Shirahama and Cohen, through an AA-amyloid formation in a macrophage research model, demonstrated amyloid fibrils arising from structures determined to be lysosomes, as they contained acid phosphatase [7,8].

Amyloid first occurs in the mesangium and vasculature containing pericytes/smooth muscle cells in the kidneys of patients with AL-amyloidosis. It has been shown that mesangial and smooth muscle cells, including pericytes, normally displaying a smooth muscle phenotype (with myofilaments and attachment plaques) transform morphologically and physiologically into a macrophage phenotype, losing their smooth muscle features, which are replaced by the appearance in the cytoplasm of mesangial cells of numerous cytoplasmic lysosomes, endowing them with the ability to become phagocytic [9]. This transformation is crucial for light-chain amyloidogenesis to take place.

Not all light chains are amyloidogenic. The physicochemical composition and conformation of various light chains are important factors in the ability of a given light chain to form amyloid. Some of these light-chain factors may be of importance in the proclivity of certain light chains to interact with caveolae at the MC surface and use the receptor sortilin (SORLI) to become internalized [1,10,11] and interact with endosomes. Endosomes then recycle the receptor to the surface of the MCs by way of vesicles that bud from them and target the plasma membrane. The receptor is returned to the cell surface for further binding and activity. How amyloid fibrils are formed in the acidic milieu of the lysosomes remained unclear until recently, when in vitro studies using MCs incubated with amyloidogenic light chains obtained and purified from the urine of patients with renal-biopsy-proven AL-amyloidosis, using gradient centrifugation technology, clearly showed how monotypical light chains interacted with endosomes and lysosomes to eventually form fibrils. Most fibrils were formed in the very acidic milieu of the late (mature) lysosomes (pH = 5), and alkalinizing (raising the pH of) the lysosomes reduced amyloid formation [12]. The accumulation of light chains in the MCs alters cell dynamics and lysosomal function, as it has been shown to occur in proximal tubulopathies associated with monoclonal light chains in proximal tubules [13]. Rab proteins are involved in the trafficking of the light chains in the endolysosomal compartment [1,2,11].

It remained to be demonstrated whether such mechanisms were also at play in the human renal mesangium. The present study identifies fibril-forming organelles (FFOs) participating in fibrillogenesis in renal biopsies from patients with AL-amyloidosis. These FFOs are labeled for lysosomal-associated membrane protein -1 (LAMP-1) and CD-68, epitopes that are displayed by mature lysosomes. The co-localization of monotypical light chains and pertinent light chains and with lysosomal-associated membrane protein, CD-68 and, most importantly, LAMP-1 in FFOs strongly supports the notion that that these FFOs with lysosomal determinants participate in the formation of fibrils. A significant number of the MCs exhibited these organelles in different stages of fibril formation. FFOs were surrounded by intra- and extracellular fibrils with a morphology and diameter typical of amyloid.

2. Material and Methods

2.1. Clinical Information

Thirteen renal biopsies from patients with AL-amyloidosis retrieved from our files were reviewed and comprise the subject of this manuscript. The patients' records were reviewed, and the information obtained is summarized in Table 1. The information compiled reflects what was available at the time of the biopsy. Some patients had an incomplete workup at that time. None of the patients were treated for plasma cell dyscrasia prior to the renal biopsies.

Table 1. Clinical features of patients in the study.

AL-Amyloidosis Cases							
Case	Age	Sex	Pertinent Clinical Presentation	Proteinuria (gm/day)	Serum Creatinine (mg/dL)	Type of LC	Multiple Myeloma at Time of Biopsy
1	73	M	Sinus Tachycardia; Nephrotic syndrome			λ	No
2	41	F	Renal failure/Proteinuria		12	Ϗ	No
3	71	F	Proteinuria; Atrial Fibrillation		0.64–0.74	λ	No
4	64	F	Nephrotic syndrome			λ	Yes
5	67	M	Proteinuria			Ϗ	No
6	70	M	Proteinuria; CKD	6	5.3	λ	No
7	64	M	Renal failure/Proteinuria		2–2.4	Ϗ	Yes
8	71	M	Nephrotic syndrome	7		λ	No
9	63	M	Nephrotic syndrome			λ	Yes
10	70	F	Proteinuria; Renal insufficiency		3.71	λ	Yes
11	75	M	Acute/Chronic kidney failure/Proteinuria			Ϗ	No
12	71	M	Waldenström macroglobulinemia/ Renal failure	4.5	1.7	Ϗ	No
13	65	F	Proteinuria; Chronic lymphocytic leukemia	13	0.83	λ	No

CKD = Chronic Kidney Disease.

The patients' ages ranged from 41 to 75 years old. Eight male and five female patients were the subjects of this study. Clinical presentation from the nephrological point of view varied from proteinuria/nephrotic syndrome (12 patients) to renal insufficiency/failure. Only 4 had a diagnosis of multiple myeloma prior to the renal biopsy, but not all the patients had a complete workup for myeloma at the time of the biopsy (Table 1). One had a diagnosis of Waldenstrom macroglobulinemia, and another had a diagnosis of chronic lymphocytic leukemia. It cannot be stated with certainty how many of these cases were monoclonal gammopathy of renal significance (MGRS), except for 4 of them with complete workup prior to renal biopsy failing to show any evidence of an underlying malignancy. Proteinuria varied from 4.5 to 13 g/day and serum creatinine ranged from 0.83 to 12 mg/dL, reflecting a wide range of chronicity.

2.2. Light Microscopy

The biopsies were fixed in formalin, embedded in paraffin, and stained with hematoxylin and eosin, periodic acid–Schiff (PAS), silver methenamine, and trichrome stains, following well-established protocols, and were examined microscopically using a BH40 Olympus light microscope. Control renal biopsies included 5 cases with the following diagnoses: minimal change disease (n = 1), membranous glomerulonephritis (n = 1), lgA nephropathy (n = 1), acute tubulointerstitial nephritis (n = 1), and diabetic nephropathy, Class IV (n = 1).

2.3. Immunofluorescence

Frozen sections from the cases delineated above were cut and stained for 9 immunoreactants: lgG, lgA, IgM, C3, Clq, albumin, fibrinogen, kappa, and lambda light chains, stained with fluorescein isothiocyanate and interpreted using a B40 Olympus microscope with fluorescence capabilities. The main aim was to identify light-chain monoclonality

associated with areas of amyloid deposition in the renal parenchyma with an emphasis on the glomeruli. Epitope retrieval was not used in any of the cases tested.

2.4. Electron Microscopy

Firstly, 1 mm cube samples of renal tissue were fixed in Karnovsky's fixative with 2.5% glutaraldehyde at pH 7.4 for at least 24 h and embedded in Epson resins. Thick sections were cut and stained with toluidine blue for identification of areas of interest to later obtain thin sections to be studied ultrastructurally. Thin sections were stained with uranyl acetate and lead citrate. Digital images were obtained, evaluated, and printed when this was deemed necessary.

2.5. Ultrastructural Immunolabeling

Thin sections placed on copper grids were etched with a 1% hydrogen peroxide solution for kappa/lambda light chains labeling and with a 1:1 solution of saturated sodium ethoxide and ethanol for lambda and CD-68 for 12 min and subsequently incubated with the following antibodies at the specified titers: kappa (1/50), lambda (1/50), LAMP-I (1/50), and CD-68 (pre-diluted) for 24 h, following a well-tested method [14]. Gold particles of 10 nm were used for the labeling procedure.

3. Results

All cases with AL-amyloidosis revealed, via light microscopy, amorphous, eosinophilic material in mesangial areas; segmentally, involving surrounding capillary walls (Figure 1A–C); and in other renal compartments.
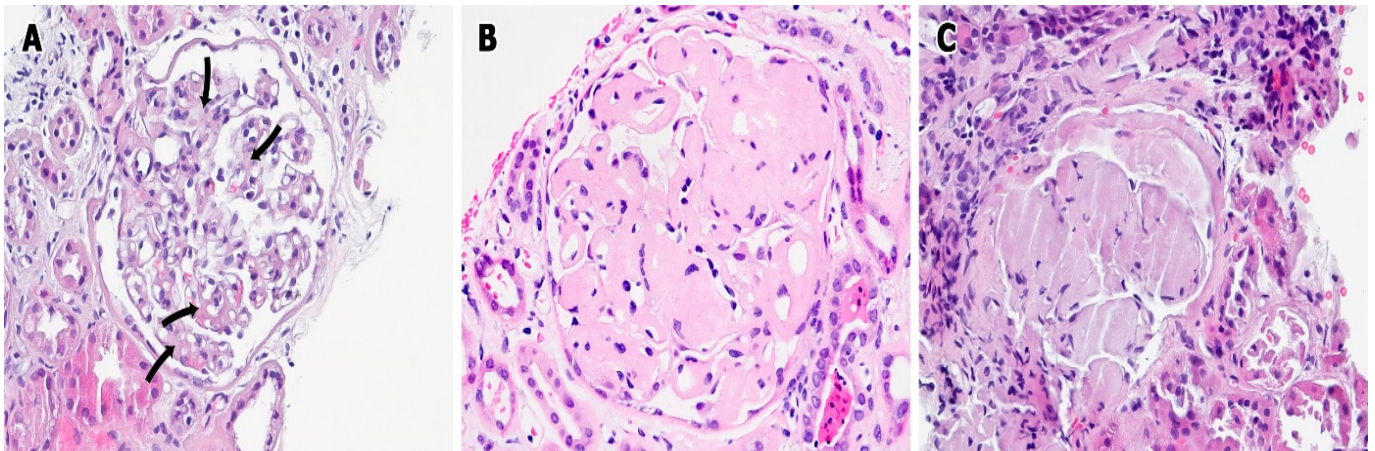
Figure 1. Magnification: (**A**) ×500, (**B**) ×500, and (**C**) ×500. Hematoxylin and eosin stain. Renal biopsy—AL-amyloidosis. Amorphous, eosinophilic material replacing mesangial areas (arrows) resulting in early, focal, and segmental deposition of amyloid: early glomerular involvement (**A**), evolving to nodular and diffuse (**B**,**C**) obliteration of the glomerular architecture and advanced glomerular involvement. Note the small number of nuclei of MCs remaining in the affected mesangium. ×—denotes the magnification for all figures.

The normal mesangium was replaced by the variably abundant fibrillary material, leaving just a few compressed MCs behind. This material deposited in the mesangium was variably (often weakly) PAS-positive but, at times, intensely positive (Figure 2A) and did not stain with the silver methenamine stain (Figure 2B, see arrows).
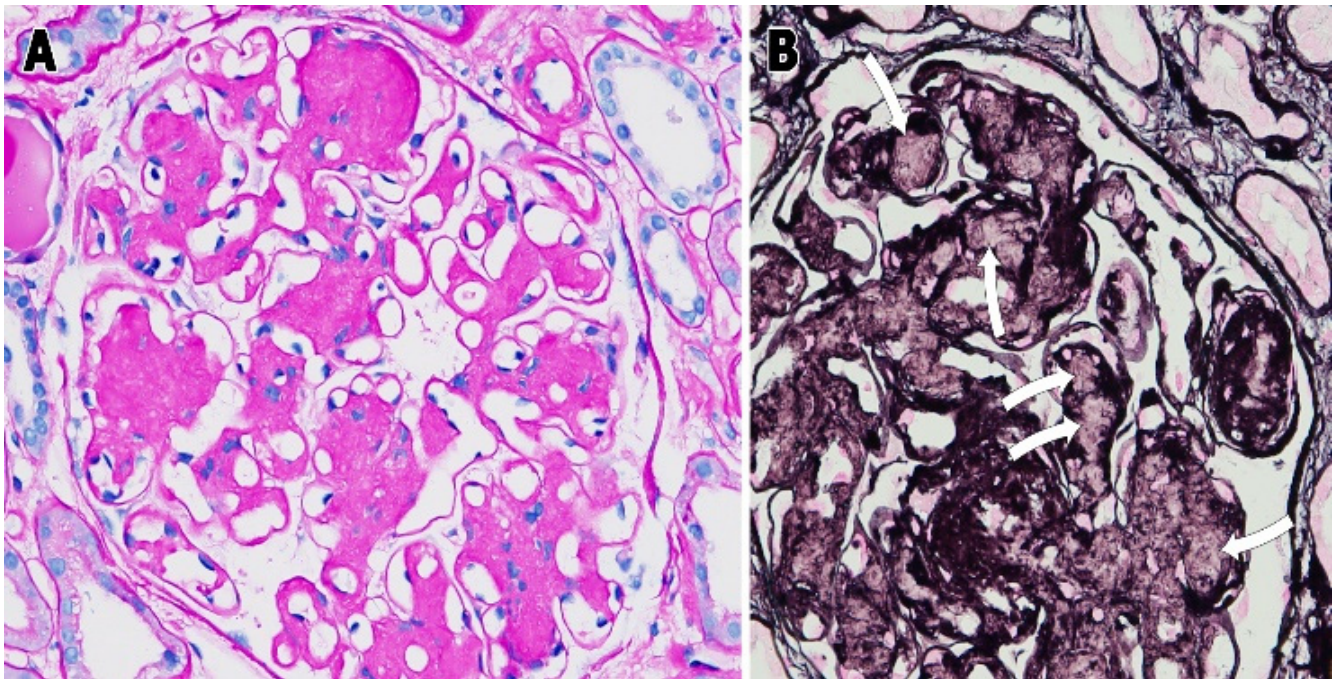
Figure 2. Magnification: (**A**) ×250 and (**B**) ×250. (**A**) Periodic acid–Schiff stain ×500; (**B**) silver methenamine stain ×500. Renal biopsy—AL-amyloidosis. In (**A**), note that the amyloid is strongly PAS positive (not common) and also, in areas with mesangial amyloid, the silver staining typical of mesangial matrix material is no longer present (arrows).

The amount of amyloid in the glomeruli varied from predominantly or almost exclusively mesangial to widespread glomerular deposition. In some cases, a distinct mesangial nodularity was appreciated (Figure 1A,C), while, in others, the amyloid deposits were more diffusely distributed (Figure 1B). The number of mesangial cells decreased as the amount of amyloid increased. The number of MCs per mesangial areas in control cases was 2.4; in early amyloidosis cases, it was 1.7; and in late cases, it was 0.8. There was also intense staining of the renal compartments involved, especially glomeruli, via the Congo red stain (Figure 3A,B), and distinct fluorescence was detected using the Thioflavin T stain in the areas with amyloid deposition (Figure 3C).
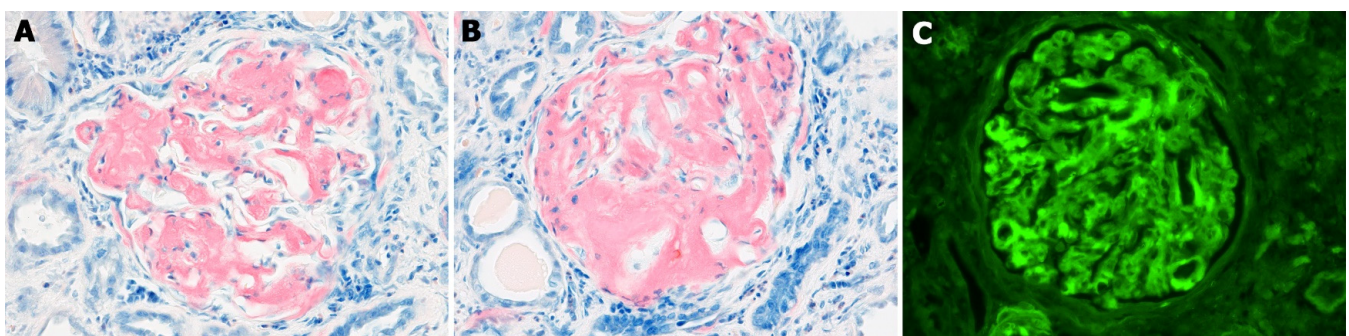
Figure 3. (**A–C**) Magnification: ×500; (**A**,**B**) are both Congo red stains, and (**C**) is a Thioflavin T stain. Two renal biopsies—AL-amyloidosis. Note congophilia in areas where amyloid is deposited. These areas were birefringent, with an apple-green appearance, when polarized. Image (**C**) shows the fluorescence of amyloid via Thioflavin T staining in a case of mesangial amyloidosis. Note the sensitivity of staining depicting small amounts of amyloid.

Via immunofluorescence, all cases of AL-amyloidosis revealed monotypical staining in areas with amyloid deposition for either kappa (n = 5) or lambda (n = 8) light chains. The stain was present in mesangial areas and peripheral capillary walls in various quantities (Figure 4A,C). The monoclonal light-chain staining was intense (3+) for the pertinent light chain and entirely negative for the other light chain. Cases with dual staining, though predominant for one of the light chains, were excluded.
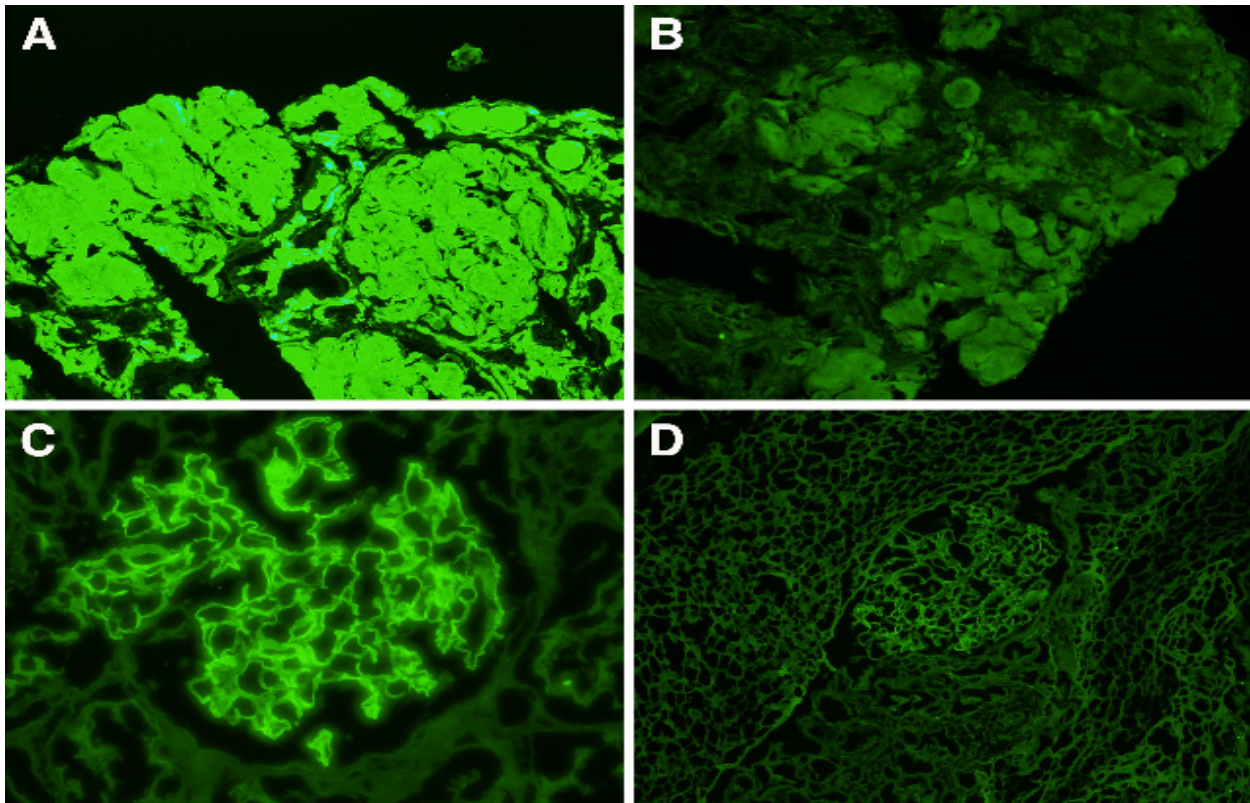
Figure 4. Magnification: (**A**) ×350, (**B**) ×350, (**C**) ×500, (**D**) ×350. Direct immunofluorescence, fluorescein isothiocyanate stain. Two renal biopsies—AL-amyloidosis. Intense staining of glomeruli and surrounding renal parenchyma (in all renal compartments) for lambda light chains in an advanced case of renal AL-amyloidosis (**A**). No staining for the kappa light chain (**B**) in the same case. Early mesangial AL-amyloidosis staining for kappa light chains (**C**) and no staining for lambda light chains (**D**) with predominant mesangial staining noted. Note the absence of staining for lambda light chains (**D**) in this second case.

No staining for any of the other immunoreactants was identified, except for focal, segmental mesangial staining for IgG in four cases.

As observed via electron microscopy, MCs were significantly decreased in numbers (especially in advanced cases), revealing prominent cup-shaped membrane indentations (caveolae/coated pits) (Figure 5). Monoclonal light chains interact with these surface caveolae, as has been demonstrated in previous immunogold labeled specimens [11], using the SORL 1 receptor. Similarly, to what was observed on the experimental platform with lysosomal gradient centrifugation [15] and abundant non-branching, randomly distributed, 6 to 13 nm fibrils were noted in the mesangium, mostly extracellularly, replacing the normal matrix. In each case, at least 50 diameters of amyloid fibrils were measured, and the mean diameter was obtained for each case.
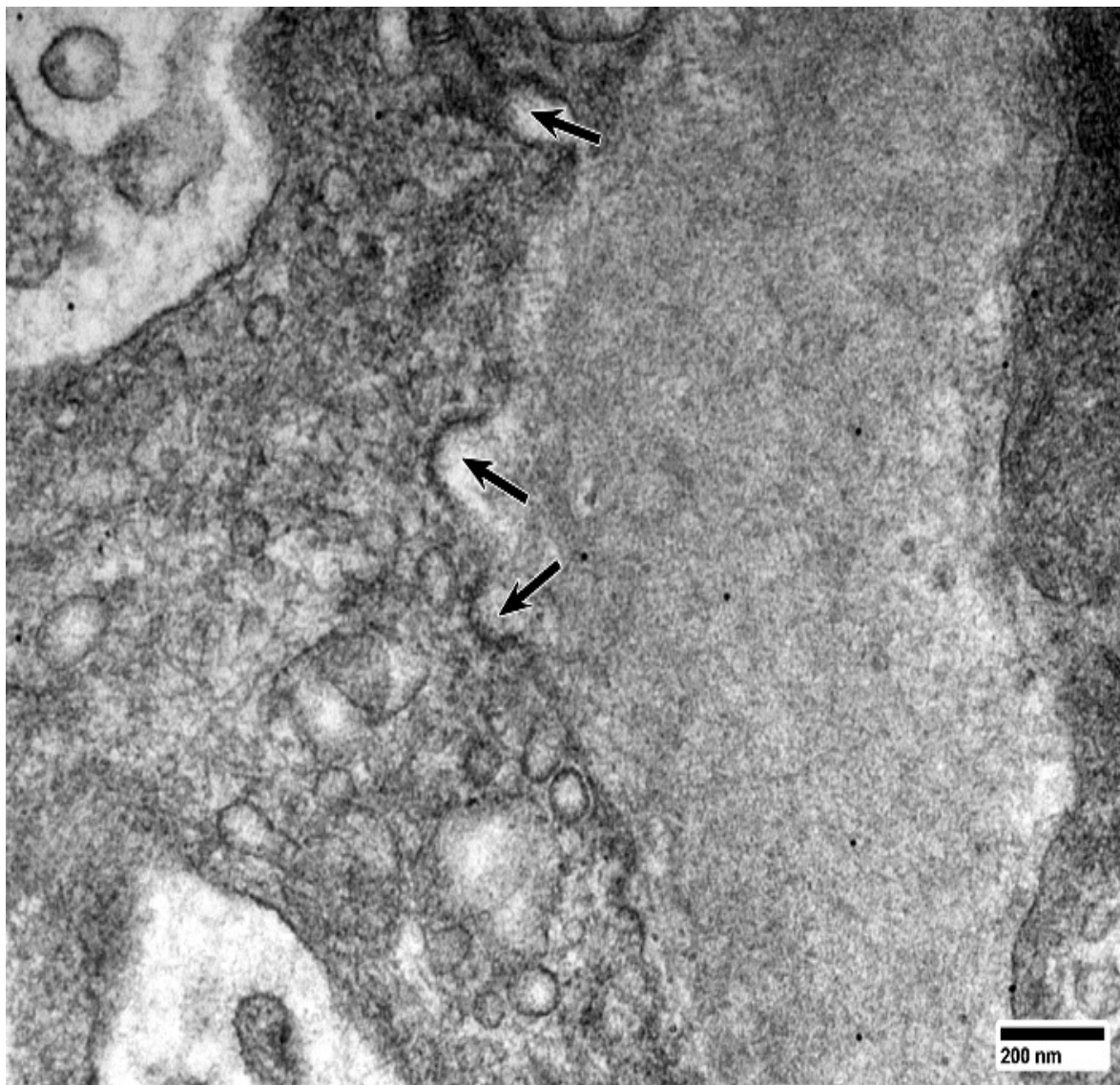
Figure 5. Magnification: ×15,000. Transmission electron microscopy. Uranyl acetate and lead citrate. Renal biopsy—AL-amyloidosis. Indentations in membranes of MCs (caveolae) (arrows) where monoclonal light chains interact with MCs and, using the receptor SORL1 located in these surface invaginations, the monoclonal light chains are internalized (endocytosed).

These fibrils were labeled for the pertinent light chain involved in amyloidogenesis (Figure 6A,B).

Findings in glomeruli and, more specifically, in the mesangium were carefully analyzed for the purpose of this study. The MCs were intimately associated with the extracellular fibrils. The MCs were noted to be in various stages of amyloid fibril formation. Their phenotypes varied from smooth muscle to macrophage, with hybrid forms noted in all cases. The majority of the MCs showed a loss of cytoplasmic myofilaments and attachment plaques replacing these with numerous lysosomes, and approximately 50% of the MCs also revealed variably sized—usually from 300 to 500 nm in diameter—organelles referred to as fibril-forming organelles (FFOs) with evidence of fibril formation inside (Figure 7A). These fibrils mostly measured from 6 to 13 nm in diameter (Figures 7A–D and 8A–D), similarly to those seen extracellularly; however, thinner fibrils corresponding to protofibrils (usual diameter: 2–7 nm) were seen in some FFOs showing early evidence of fibrillogenesis.
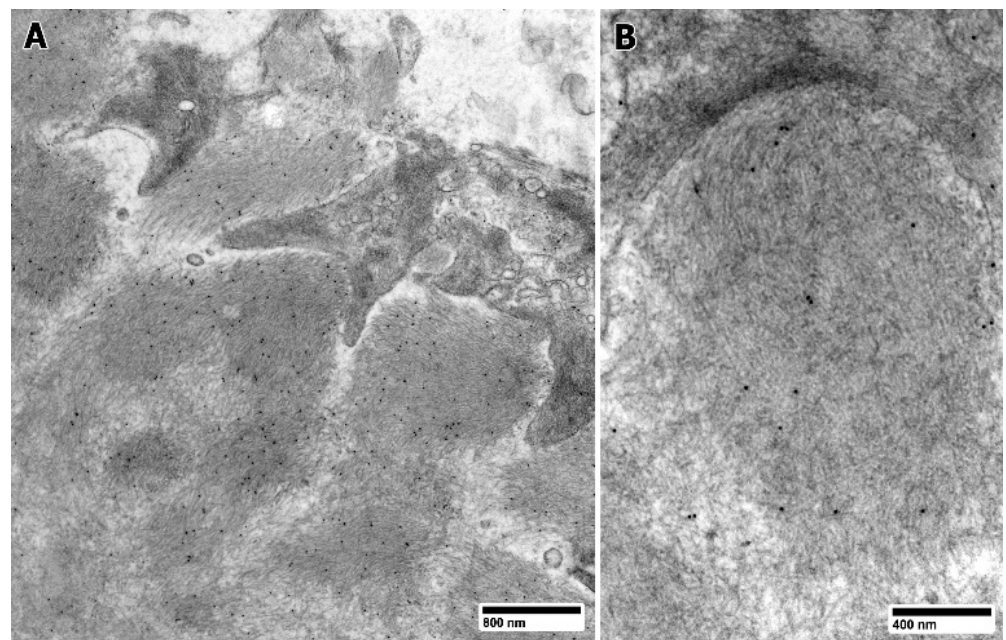
Figure 6. Magnification: (**A**) ×5000 and (**B**) ×16,000. Immunogold labeling for lambda light chains, 10 nm gold particles. Renal biopsy—AL-amyloidosis. Labeling of amyloid fibrils in the extracellular spaces for lambda light chains (fibril precursor) is noted. The fibrillary appearance of amyloid is best seen in (**B**), where fibrils are also labeled for lambda light chains (round gold particles).
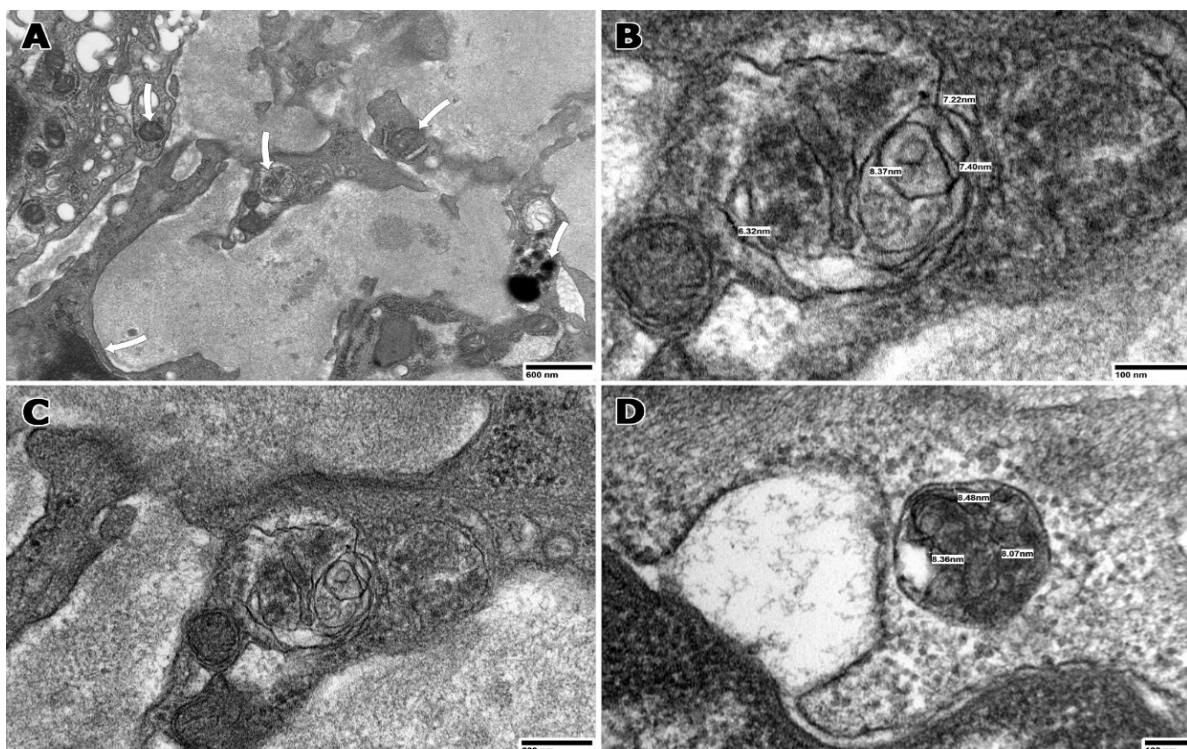
Figure 7. Magnification (**A**): ×5000, (**B**) ×15,000, (**C**) ×25,000, (**D**) ×30,000. Transmission electron microscopy, uranyl acetate, and lead citrate. Renal biopsy—AL-amyloidosis. Numerous FFOs in the cytoplasm of MCs (arrows) in (**A**). (**B**–**D**) Details of FFOs with alternating electron-dense and lucent areas and with internal fibrils measuring 6–13 nm in diameter, frequently aligned along the limiting membranes of the FFOs.
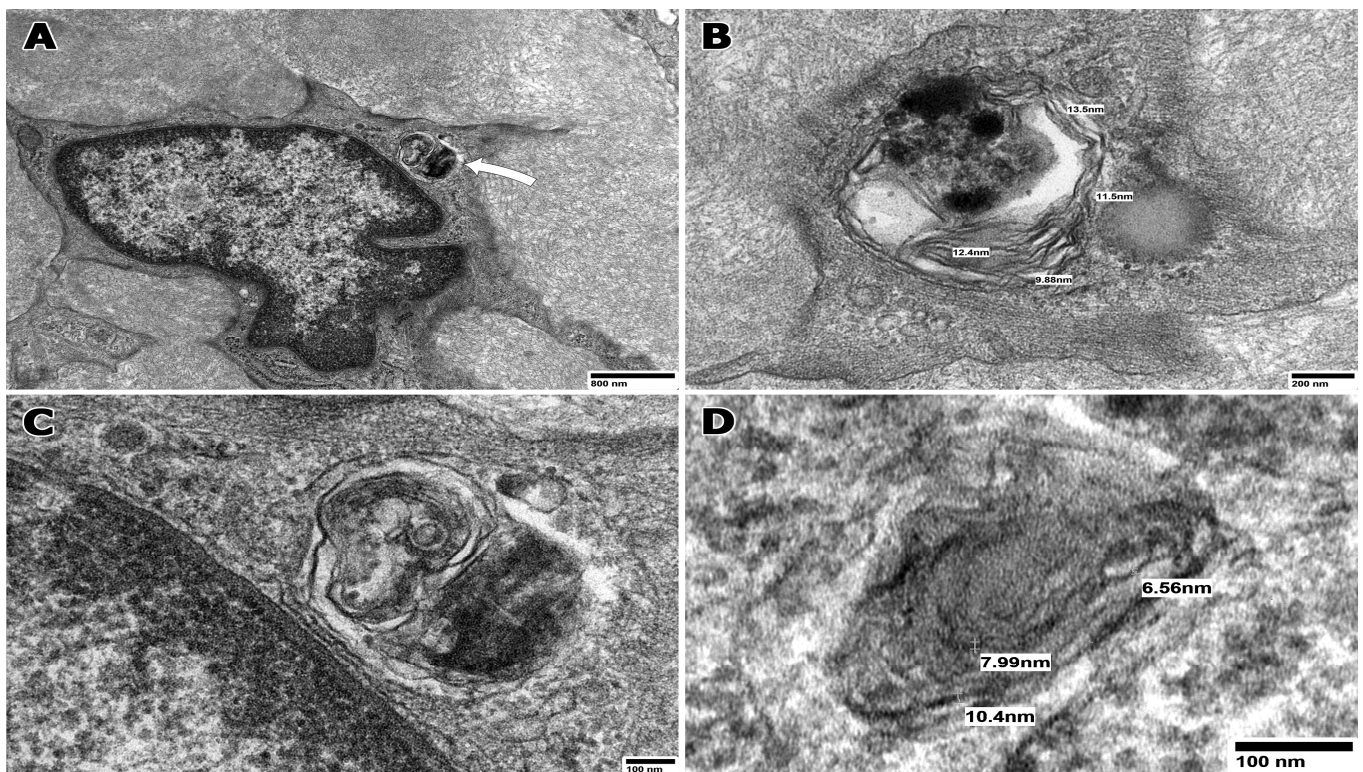
Figure 8. Magnification (**A**): ×6000, (**B**) ×15,000, (**C**) ×30 000, (**D**) ×25,000. Transmission electron microscopy. Uranyl acetate and lead citrate. Renal biopsy—AL-amyloidosis. Details of the internal composition of FFOs (arrows) from different cases. Note their proximity to the membranes of MCs. All of the FFOs contain fibrils inside. The amount and disposition of the fibrils in the FFOs are somewhat variable, though their diameter remains constant (from 6 to 13 nm) within the expected range of amyloid fibrils.

The mean number of FFOs in MCs was 3. The FFOs displayed variable electron densities inside. The fibrils were usually arranged in circular profiles around the FFOs' external limiting membranes and aligned along the limiting membranes of the organelles (Figures 7B–D and 8B–D). In some FFOs, the fibrils were in a disordered arrangement. These FFOs were commonly near or immediately adjacent to the mesangial cell membranes, where their mean diameter was 7.2 nm. Intracellular amyloid fibrils were also noted adjacent to the FFOs in occasional MCs. Not all identifiable lysosomes morphologically present in MCs were seen engaged in fibrillogenesis, even in cells where focal fibril formation was evident in FFOs. The fibril diameters are shown.

Ultrastructural labeling for monotypical kappa/lambda light chains (Figure 9) and lysosomal antigen membrane protein-I (LAMP-I) (Figure 10A,B) and CD68 (Figure 11) demonstrated labeling of the FFOs.

There was also labeling for the pertinent light chains of the amyloid fibrils in their various locations (Figure 8A–D).
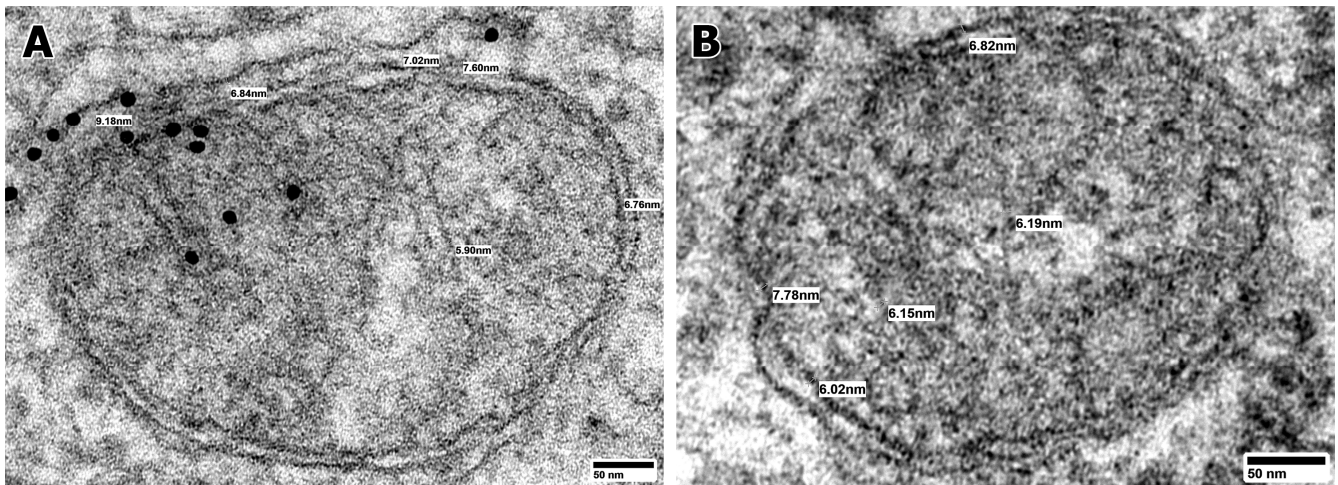
Figure 9. Magnification: (**A**) ×60,000, (**B**) ×60,000. Immunogold labeling for (**A**) lambda, (**B**) kappa, 10 nm gold particles. Transmission electron microscopy. Uranyl acetate and lead citrate. Gold immunolabeling—10 nm gold particles. Uranyl acetate and lead citrate stain. Renal biopsy—AL-amyloidosis. Labeling of the FFOs for lambda light chains (**A**) indicating derivation from lambda light chains. Note absent labeling for kappa light chains (**B**) in immunolabeled samples.
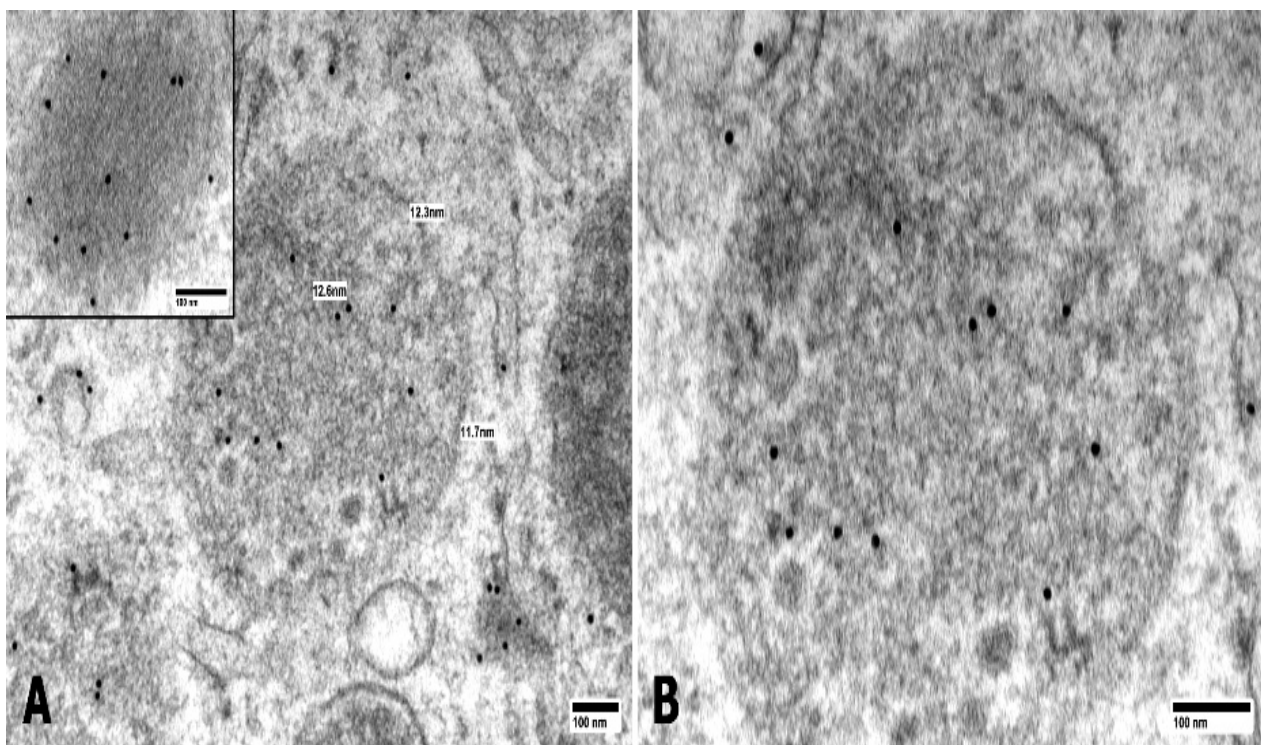
Figure 10. Magnification: (**A**) ×25,000 (insert, ×40,000), (**B**) ×40,000. Transmission electron microscopy. Uranyl acetate and lead citrate. Immunogold labeling for lysosomal antigen membrane protein (LAMP)—10 nm gold particles. Renal biopsy—AL-amyloidosis. Note distinct labeling for LAMP-I in lysosomes containing fibrils in MCs. No background labeling.
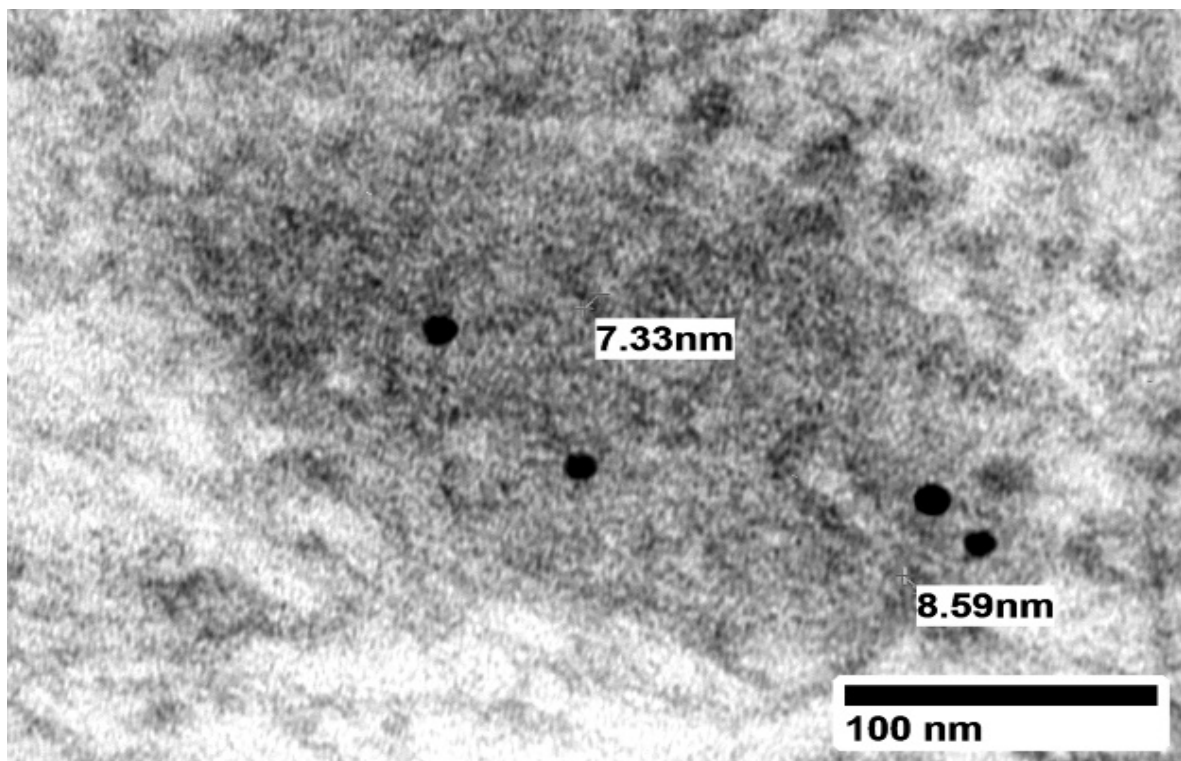
Figure 11. Magnification: ×40,000. Transmission electron microscopy. Uranyl acetate and lead citrate. Immunogold labeling for CD-68—10 nm gold particles. Renal biopsy—AL-amyloidosis. FFOs in MCs are labeled for CD-68 as well. Note fibrils inside FFO.

4. Discussion

Decades ago, Von Gise et al. highlighted the fundamental role of the mesangium in early amyloidosis [16]. At the time, they concluded that the amyloid was formed in the extracellular space from amyloid precursors brought via the bloodstream under the influence of lysosomal enzymes released from epithelial, mesangial, and perhaps endothelial cells. Indeed, the mesangium represents the first glomerular location in which renal amyloid is found in patients with AL-amyloidosis. Today, the concept that MCs play a crucial role in the beginning and progression of renal amyloidosis prevails.

More recent studies have shown that fibril formation begins intracellularly in the endosomes (pH of about 6) in MCs very soon after the endocytosis of the monoclonal light chains into MCs. However, it is in the late (mature) lysosomal compartment where light-chain processing and fibril formation are mainly carried out [15].

In 1973, Linke et al. reported the formation of amyloid fibrils by digesting light chains with proteolytic enzymes [17]. Furthermore, Epstein et al. digested light chains in vitro with human kidney lysosomal enzymes forming amyloid fibrils the following year [18], solidifying the role of kidney enzymes in amyloid formation.

The exocytosis of fibrils into the extracellular compartment has been documented, using scanning electron microscopy, as occurring when lysosomes approach the mesangial cell membranes delivering the fibrils to the outside, primarily by means of gaps in the cell membranes [19]. Once fibrils reach the extracellular space, they may promote seeding and rapid expansion of the amyloid load in the tissue. While there may be other mechanisms involved in the delivery of fibrils and the progression of amyloidosis, the present study highlights how fibrils are formed in the MCs as the initiating event in AL-amyloidogenesis. Amyloid in the extracellular space additionally promotes enhancements in the activity of matrix metalloproteinases and the destruction of the native mesangial matrix rich in collagen IV, eventually replacing entire mesangial areas [20], as well as inhibiting transforming growth factor-B, which impairs the repair of the replaced matrix.

Lysosomes encompass a heterogeneous group of membrane-limited vesicles, differing in size and density, characterized by de Duve in the 1950s [21]. The lysosomes contain glycosidases, sulfatases, and proteases functioning in the active processing and degradation of intracellular products [22].

FFOs are organelles with a unique appearance but with features of lysosomes, which engage in the processing of light chains that become internalized into MCs. They have a typical ultrastructural appearance that separates them from the more characteristic appearance of lysosomes. Whether the function of FFOs is restricted with amyloid fibril formation remains to be investigated and, if this is not the case, could they also be associated with the fibrils formed in fibrillary glomerulonephritis? While lysosomal appearance in general can be quite diverse, including recognized primary and secondary forms, and their function is also quite heterogeneous. On the other hand, in the general category of lysosomes, FFOs remain unique in terms of their overall appearance, with an internal composition wherein fibrils are identified together with alternating electron-dense and lucent areas, the latter probably representing where enzymes were located at one time and have been extruded and consumed in the process. FFOs may represent a specific type of lysosome, with the main function of fibrillogenesis or, otherwise, normal lysosomes reprogrammed to engage in fibril formation. These structures belong to what is referred to as the post-lysosomal compartment, where non-fully digestible material accumulates [23].

Significant advances have taken place in examining the physicochemical characteristics of the light chains responsible for their amyloidogenicity, but much work remains to be undertaken. From the initial work by Solomon et al. [23] identifying lambda light chains as more prone to be associated with amyloidosis than kappa light chains, to the finding of lambda VI light-chain tropism for renal amyloid [24,25], to the more advanced studies dealing with specific physicochemical characteristics (amino acid abnormalities) in the composition and configuration of light chains [10], rendering them prone to being associated with amyloid fibril formation, the field has matured significantly.

5. Conclusions

This ultrastructural/immunolabeling study demonstrates the intracellular formation of amyloid fibrils with characteristics of amyloid fibrils in FFOs in MCs in renal biopsies from patients with renal AL-amyloidosis. The lysosomal environment with a markedly acidic pH provides the perfect milieu for light-chain processing into fibrils. Chloroquine is known to inhibit the acidification of the endolysosomal compartment and reduce amyloid formation in MCs [12]. Clinical materials (renal biopsies) recapitulated the in vitro findings, emphasizing the unique value of this translational study when it comes to progressing our understanding of amyloidogenesis from animal models [26] to humans. This work provides a better understanding of the process of fibrillogenesis in mesangial cells, which is crucial to devising therapeutic advances to treat AL-amyloidosis.

Author Contributions: Conceptualization, G.A.H., E.A.T.-H., J.T., and L.D.P.-Y.; methodology, G.A.H. and B.L.; validation, G.A.H. and B.L.; formal analysis, G.A.H., E.A.T.-H., L.D.P.-Y., J.T., and C.Z.; investigation, G.A.H., E.A.T.-H., L.D.P.-Y., C.Z. and B.L.; resources, G.A.H. and E.A.T.-H.; data curation, G.A.H., L.D.P.-Y., E.A.T.-H. and J.T.; writing—original draft preparation, G.A.H.; writing—review and editing, G.A.H. and J.T.; visualization, G.A.H.; supervision, G.A.H.; project administration, G.A.H.; funding acquisition, G.A.H. All authors have read and agreed to the published version of the manuscript.

Institutional Review Board Statement: Ethical review and approval were waived for this study, due to the retrospective character of the study and data anonymization.

Informed Consent Statement: Patient consent was waived due to the retrospective character of the study and data anonymization.

References

1. Herrera, G.A.; Teng, J.; Turbat-Herrera, E.A.; Zeng, C.; Del Pozo-Yauner, L. Understanding Mesangial Pathobiology in AL-Amyloidosis and Monoclonal Ig Light Chain Deposition Disease. *Kidney Int. Rep.* **2020**, *5*, 1870–1893. [CrossRef] [PubMed]
2. Herrera, G.A. Renal amyloidosis: Pathogenesis. *Ultrastruct. Pathol.* **2021**, *45*, 267–275. [CrossRef] [PubMed]
3. Sirac, C.; Herrera, G.A.; Sanders, P.W.; Batuman, V.; Bender, S.; Ayala, M.V.; Javaugue, V.; Teng, J.; Turbat-Herrera, E.A.; Cogné, M.; et al. Animal models of monoclonal immunoglobulin-related renal diseases. *Nat. Rev. Nephrol.* **2018**, *14*, 246–264. [CrossRef]
4. Martinez-Rivas, G.; Bender, S.; Sirac, C. Understanding AL amyloidosis with a little help from in vivo models. *Front. Immunol.* **2022**, *13*, 1008449. [CrossRef]
5. Picken, M.M. The pathology of amyloidosis in classification: A review. *Acta Haematol.* **2020**, *143*, 322–334. [CrossRef] [PubMed]
6. Herrera, G.A. Plasticity of mesangial cells: A basis for understanding pathological alterations. *Ultrastruct Pathol.* **2006**, *30*, 471–479. [CrossRef]
7. Shirahama, T.; Cohen, A.S. An analysis of the close relationship of lysosomes to early deposits of amyloid. Ultrastructural evidence in experimental mouse amyloidosis. *Am. J. Pathol.* **1973**, *73*, 97–114.
8. Shirahama, T.; Cohen, A.S. Intralysosomal formation of amyloid fibrils. *Am. J. Pathol.* **1975**, *81*, 101–116.
9. Keeling, J.; Teng, J.; Herrera, G.A. AL-amyloidosis and light-chain deposition disease light chains induce divergent phenotypic transformations of human mesangial cells. *Lab. Investig.* **2004**, *84*, 1322–1338. [CrossRef]
10. Del Pozo-Yauner, L.; Turbat-Herrera, E.A.; Pérez-Carre6n, J.; Herrera, G.A. From the Light Chain Sequence to the Tissue Microenvironment: Contribution of the Mesangial Cells to Glomerular Amyloidosis. *Hemato* **2022**, *3*, 232–267. [CrossRef]
11. Herrera, G.A.; Del Pozo-Yauner, L.; Teng, J.; Zeng, C.; Shen, X.; Moriyama, T.; Ramirez Alcantara, V.; Liu, B.; Turbat-Herrera, E.A. Glomerulopathic light chain-mesangial cell interactions: Sortilin-related receptor (SORLI) and signaling. *Kidney Int. Rep.* **2021**, *6*, 1379–1396. [CrossRef]
12. Isaac, J.; Kerby, J.D.; Russell, W.; Dempsey, S.C.; Sanders, P.W.; Herrera, G.A. In-vitro modulation of AL-amyloid formation by human mesangial cells exposed to amyloidogenic light chains. *Amyloid Int. J. Exp. Clin. Investig.* **1998**, *5*, 238–246. [CrossRef] [PubMed]
13. Luciani, A.; Sirac, C.; Terryn, S.; Javaugue, V.; Prange, J.A.; Bender, S.; Bonaud, A.; Cogné, M.; Aucouturier, P.; Ronco, P.; et al. Impaired lysosomal function underlies monoclonal light chain-associated Renal Fanconi Syndrome. *J. Am. Soc. Nephrol.* **2016**, *27*, 2049–2061. [CrossRef]
14. Mai, H.L.; Sheikh-Hamad, D.; Herrera, G.A.; Gu, X.; Truong, L.D. Immunoglobulin heavy chain can be amyloidogenic: Morphologic characterization including immunoelectron microscopy. *Am. J. Surg. Pathol.* **2003**, *27*, 541–545. [CrossRef]
15. Herrera, G.A.; Teng, J.; Zeng, C.; Pozo-Yauner, L.D.; Liu, B.; Turbat-Herrera, E.A. AL(light chain)-amyloidogenesis by mesangial cells involves active participation of lysosomes: An ultrastructural study. *Heliyon* **2023**, *9*, e15190. [CrossRef] [PubMed]
16. von Gise, H.; Christ, H.; Bohle, A. Early glomerular lesions in amyloidosis. Electronmicroscopic findings. *Virchows Arch. A Pathol. Anat. Histopathol.* **1981**, *390*, 259–272. [CrossRef] [PubMed]
17. Linke, R.P.; Zucker-Franklin, D.; Franklin, E.D. Morphologic, chemical, and immunologic studies of amyloid-like fibrils formed from Bence Jones Proteins by proteolysis. *J. Immunol.* **1973**, *111*, 10–23. [CrossRef]
18. Epstein, W.V.; Tan, M.; Wood, I.S. Formation of "amyloid" fibrils in vitro by action of human kidney lysosomal enzymes on Bence Jones proteins. *J. Lab. Clin. Med.* **1974**, *84*, 107–110.
19. Teng, J.; Turbat-Herrera, E.A.; Herrera, G.A. Extrusion of amyloid fibrils to the extracellular space in experimental mesangial AL-amyloidosis: Transmission and scanning electron microscopy studies and correlation with renal biopsy observations. *Ultrastruct Pathol.* **2014**, *38*, 104–115. [CrossRef]
20. Keeling, J.; Herrera, G.A. Matrix metalloproteinases and mesangial remodeling in light chain-related glomerular damage. *Kidney Int.* **2005**, *68*, 1590–1603. [CrossRef]
21. De Duve, C.; Watt-iaux, R. Functions of lysosomes. *Annu. Rev. Physiol.* **1966**, *28*, 435–492. [CrossRef] [PubMed]
22. Müller, S.; Dennemärker, J.; Reinheckel, T. Specific functions of lysosomal proteases in endocytic and autophagic pathways. *Biochim. Biophys. Acta* **2012**, *1824*, 34–43. [CrossRef] [PubMed]
23. Hirota, Y.; Masuyama, N.; Kuronita, T.; Fujita, H.; Himeno, M.; Tanaka, Y. Analysis of post-lysosomal compartments. *Biochem. Biophys. Res. Commun.* **2004**, *314*, 306–312. [CrossRef] [PubMed]
24. Solomon, A.; Frangione, B.; Franklin, E.C. Bence Jones proteins and light chains of immunoglobulins. Preferential association of the V lambda VI subgroup of human light chains with amyloidosis AL (lambda). *J. Clin. Investig.* **1982**, *70*, 453–460. [CrossRef] [PubMed]

25. Comenzo, R.L.; Zhang, Y.; Martinez, C.; Osman, K.; Herrera, G.A. The tropism of organ involvement in primary systemic amyloidosis: Contributions of Ig V(L) germ line gene use and clonal plasma cell burden. *Blood* **2001**, *98*, 714–720. [CrossRef]
26. Teng, J.; Turbat-Herrera, E.A.; Herrera, G.A. An animal model of glomerular light-chain-associated amyloidogenesis depicts the crucial role of lysosomes. *Kidney Int.* **2014**, *86*, 738–746. [CrossRef]